GBA 3

Cinétique enzymatique

Support graphique aux notes de cours

Z.GUNATA

Microorganismes	Enzymes	Classe.	Exemples applications
Arthrobacter	glucose isomérase	5.3.1.5.	alimentation (boissons)
Bacillus cereus	protéase β-amylase isoamylase	3.4.24.4. 3.2.1.2. 3.2.1.68.	boissons céréales, boissons céréales, boissons
Bacillus coagulans	glucose isomérase	5.3.1.5.	céréales, fruits
Bacillus licheniformis	α -amylase protéase	3.2.1.1. 3.4.24.4.	céréales, boissons, patisserie viandes, poissons, boissons
Bacillus megatherium	β-amylase	3.2.1.2.	céréales, boissons
Bacillus subtilis	α-amylase β-amylase endo β-glucanase hémicellulase protéase	3.2.1.1. 3.2.1.2. 3.2.1.6. 3.2.1.78. 3.4.24.4.	céréales, fruits, miel céréales, boissons boissons chocolat, thé, café boissons, patisserie
Leuconostoc cenos	décarboxylase	1.1.1.39.	boissons
Micrococcus lysodeiticus	catalase	1.11.1.6.	lait, fromage, œufs
Actinomycètes *Streptomyces albus* *Streptomyces olivaceus* *Streptomyces rubiginosus* *Streptomyces sp.*	 glucose-isomérase glucose-isomérase glucose-isomérase xylanase	 5.3.1.5. 5.3.1.5. 5.3.1.5. 3.2.1.32.	 céréales, fruits, légumes, boissons (bière, vins), sucre, miel céréales, boissons (bière, vins), thé, chocolat, café
champignons microscopiques	**activité enzymatique**	**classification**	**exemples d'applications**
Aspergillus oryzae	α-amylase amyloglucosidase cellulase hémicellulase lipase maltase pectinase protéase	3.2.1.1. 3.2.1.3. 3.2.1.4. 3.2.1.70. 3.1.1.3. 3.2.1.20. 3.2.1.15. 3.4.23.6.	céréales, patisserie fruits, boissons, sucre, miel fruits, légumes, boissons chocolat, café, thé fromages, fruits, huile céréales graisses, huiles, fruits fromages, viandes, poissons
Aspergillus niger	α-amylase glucoamylase cellulase lipase cellobiase lactase invertase pectinase	3.2.1.1. 3.2.1.3. 3.2.1.4. 3.1.1.3. 3.2.1.21. 3.2.1.23. 3.2.1.26. 3.2.1.15.	céréales, fruits, boissons fruits, boissons, sucre, miel fruits, boissons fromages, graisses, fruits fruits, végétaux laits, fromages graisses, huiles, boissons
levures	**activité enzymatique**	**classification**	**exemples d'applications**
Candida lipolytica	lipase	3.1.1.3.	
Saccharomyces cerevisae *Saccharomyces carbobergensis*	invertase invertase et α-galactosidase	3.2.1.26. 3.2.1.26. 3.2.1.22.	confiserie confiserie sucre et miel
Kluyveromyces fragilis	lactase involinase invertase	3.2.1.23. 3.2.1.7. 3.2.1.26.	laits, fromages sucre, miel confiserie
Kluyveromyces lactis	lactase	3.2.1.23	laits, fromages, glaces

Figure I.2 ... alimentaire et leur origine

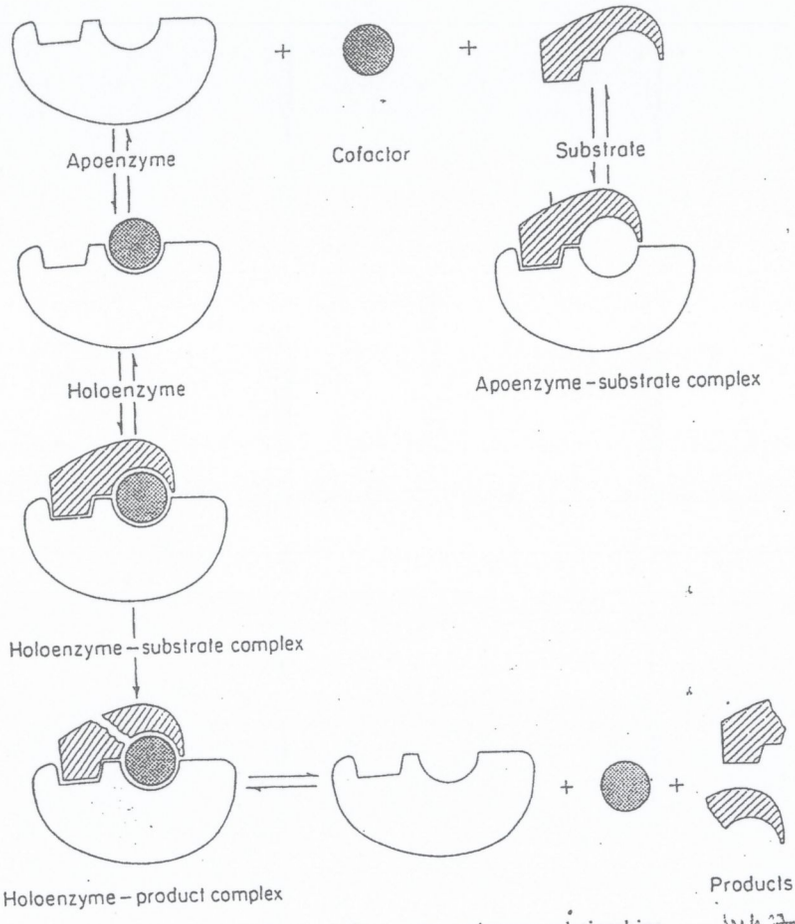

Figure 4 Apoenzyme–cofactor–holoenzyme–substrate relationships. Whitaker, 1994

Représentation selon Lineweaver et Burk : $\frac{1}{v} = f(\frac{1}{[S]})$

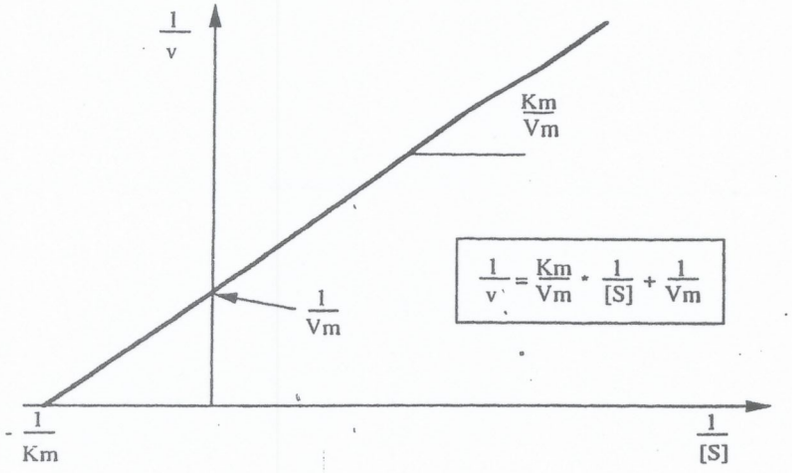

Représentation selon Eadie et Hofstee : $v = f(\frac{v}{[S]})$

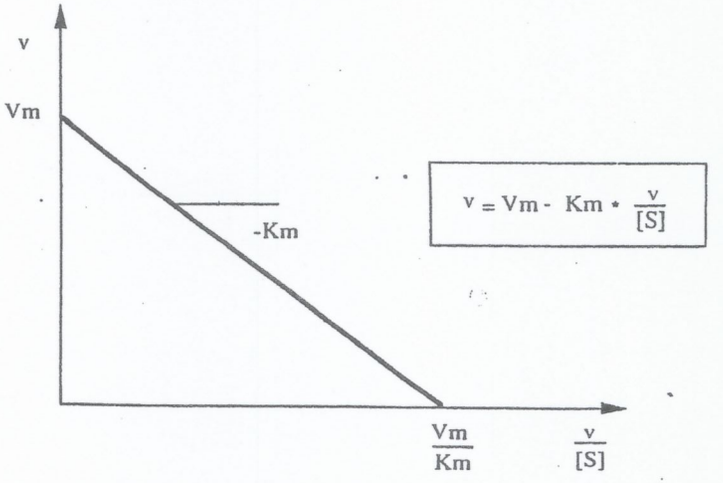

Représentation selon Hanes-Woolf : $\frac{[S]}{v} = f([S])$

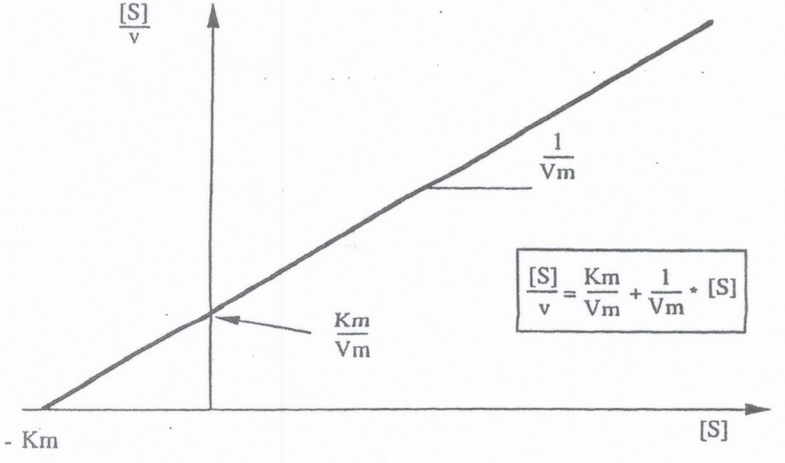

Représentation linéaire directe :

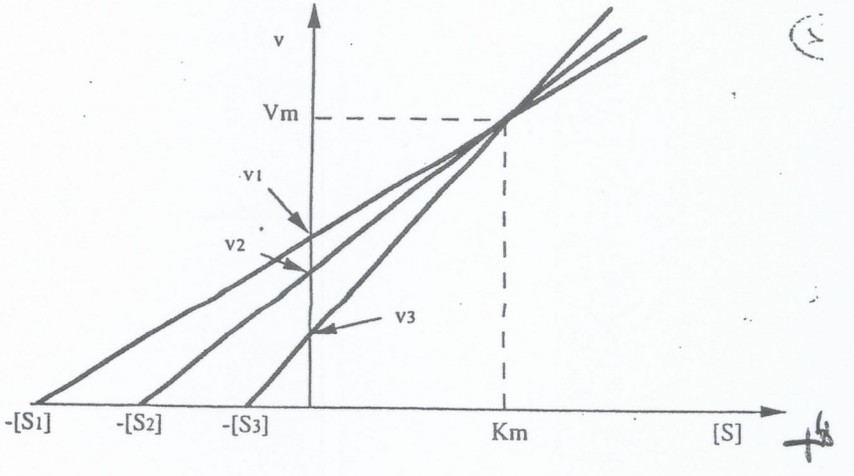

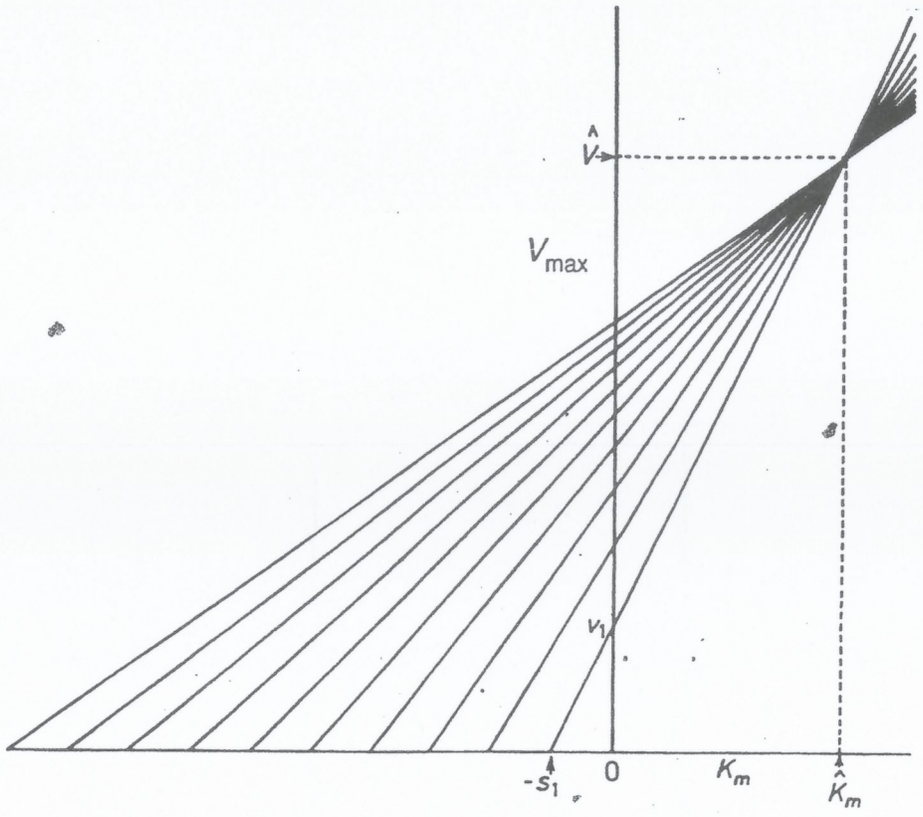

Figure 2. The direct linear plot of data that fits Equation 1 exactly (7, 8, 17).

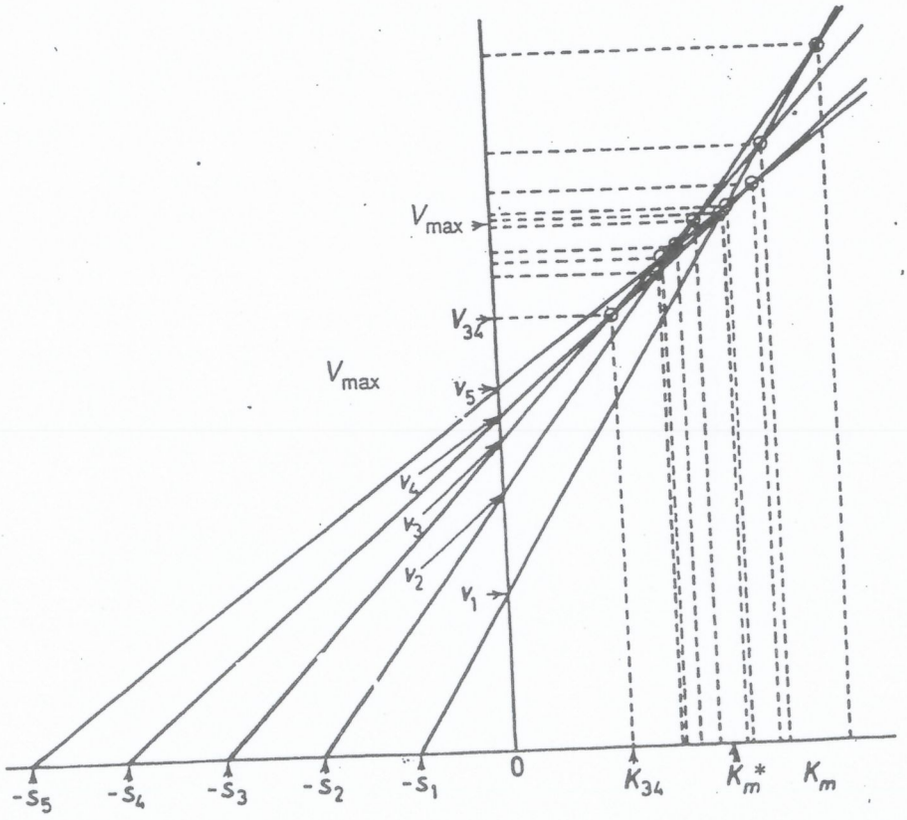

Figure 3. The direct linear plot of data containing errors. K_m^* and V_{max}^* are the median, best-fit, values (7, 8, 17).

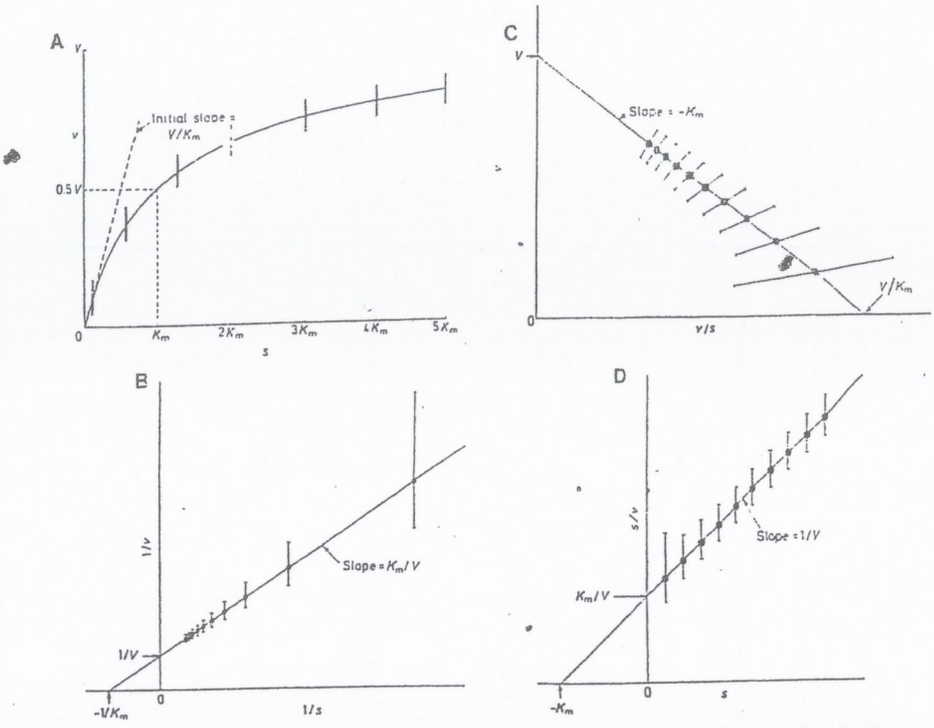

Figure 8 Effect of errors in velocity measurements on the estimation of V_{max} and K_m by linear plots. (A) Original data for velocity as a function of substrate concentration assuming an error in measurement of 5% of V_{max}. (B) Linear transformation of the original data to Lineweaver–Burke plot. (C) Eadie–Scatchard plot. (D) Hanes–Woolf plot. (Reprinted from Cornish-Bowden, 1979, with permission.)

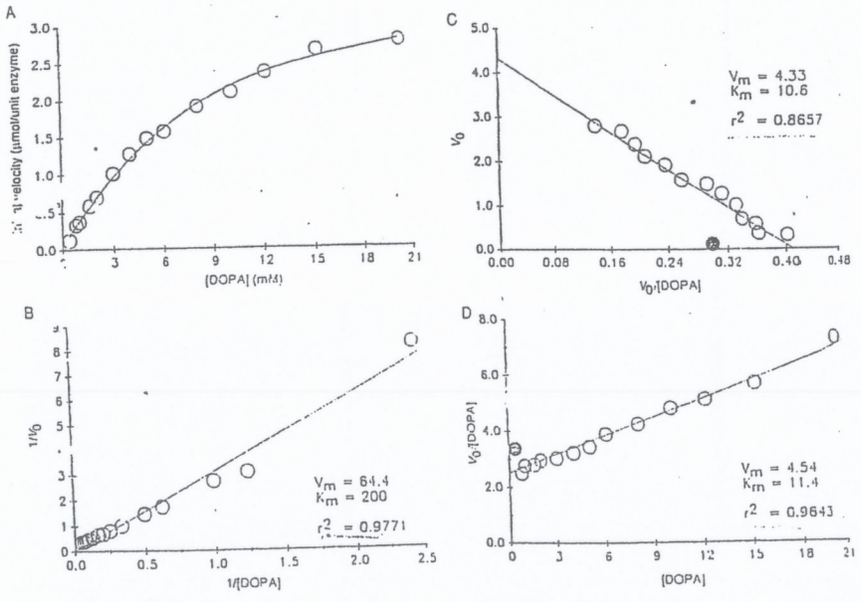

Figure 9 Estimation of V_{max} and K_m of *o*-diphenol oxidase action on 3,4-dihydroxyphenylalanine (DOPA). (A) Velocity as a function of DOPA concentration. (B), (C), and (D) Linear transformation of the original data to Lineweaver–Burke, Eadie–Scatchard, and Hanes–Woolf plots, respectively. The lines were fitted by linear regression to yield estimates of V_{max} and K_m. Filled circles indicate outlying points. (Data from Fukagawa *et al.*, 1985.)

V. Hofkes, 1994

Tableau IX : Hydrolyse de différents hétérosides par la rhamnosidase, isolée de la préparation commerciale Pectinase d'*A. niger*.

Substrat	V_M ($\mu M.min^{-1}$)	k_M (mM)	Efficacité catalytique (min^{-1})	%
Naringine	66	0,045	1,46	100
Hespéridine	624	0,96	0,65	44,3
Rutinoside de phényl-2-éthyle	558	0,986	0,57	38,6
Rutinoside de linalyle	316	1,25	0,25	17,2
Rutine	1000	4,9	0,20	13,9
Rutinoside de géranyle	1379	9,96	0,14	9,4
Rutinoside de néryle	1083	7,9	0,14	9,4
Rutinoside d'α-terpinyle	333	5	0,07	4,5
α-L-rhamnopyranoside de p-nitrophényle	80	1,40	0,057	3,9
Rutinoside de benzyle	Très faible hydrolyse			
α-L-rhamnopyranoside de méthyle	Pas d'hydrolyse			

Etapes de purification	Activité totale nkatal	Protéines totales mg	Rendement en activité %	Activité spécifique nkat/mg	Facteur de purification
Préparation enzymatique initiale	3780	480	100	7,9	1
Chromatographie d'exclusion sur Ultrogel AcA44	998	3,84	26,4	260	33
Chromatographie d'échange d'ions sur DEAE Sepharose CL6B	297	1,38	7,9	216	27

Tableau VI : Bilan de purification de la β-apiosidase de la préparation enzymatique N°5.

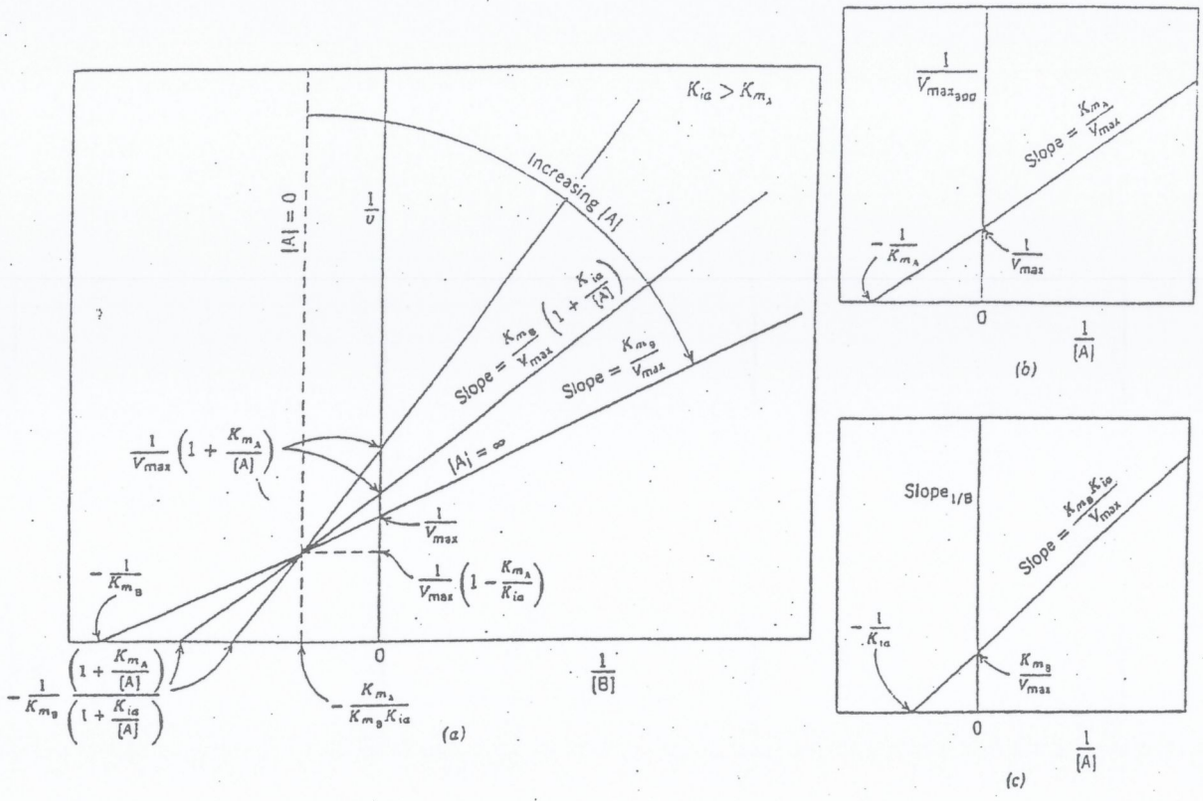
$K_{ia} > K_{m_A}$
Increasing [A]
$\frac{1}{v}$
$[A] = 0$
$[A] = \infty$
Slope $= \frac{K_{m_B}}{V_{max}}\left(1 + \frac{K_{ia}}{[A]}\right)$
Slope $= \frac{K_{m_B}}{V_{max}}$
$\frac{1}{V_{max}}\left(1 + \frac{K_{m_A}}{[A]}\right)$
$\frac{1}{V_{max}}$
$\frac{1}{V_{max}}\left(1 - \frac{K_{m_A}}{K_{ia}}\right)$
$-\frac{1}{K_{m_B}}$
$-\frac{\left(1 + \frac{K_{m_A}}{[A]}\right)}{\left(1 + \frac{K_{ia}}{[A]}\right)}$
$-\frac{K_{m_A}}{K_{m_B} K_{ia}}$
0
$\frac{1}{[B]}$
(a)
$\frac{1}{V_{max_{app}}}$
Slope $= \frac{K_{m_A}}{V_{max}}$
$-\frac{1}{K_{m_A}}$
$\frac{1}{V_{max}}$
0
$\frac{1}{[A]}$
(b)
Slope $_{1/B}$
Slope $= \frac{K_{m_B} K_{ia}}{V_{max}}$
$-\frac{1}{K_{ia}}$
$\frac{K_{m_B}}{V_{max}}$
0
$\frac{1}{[A]}$
(c)

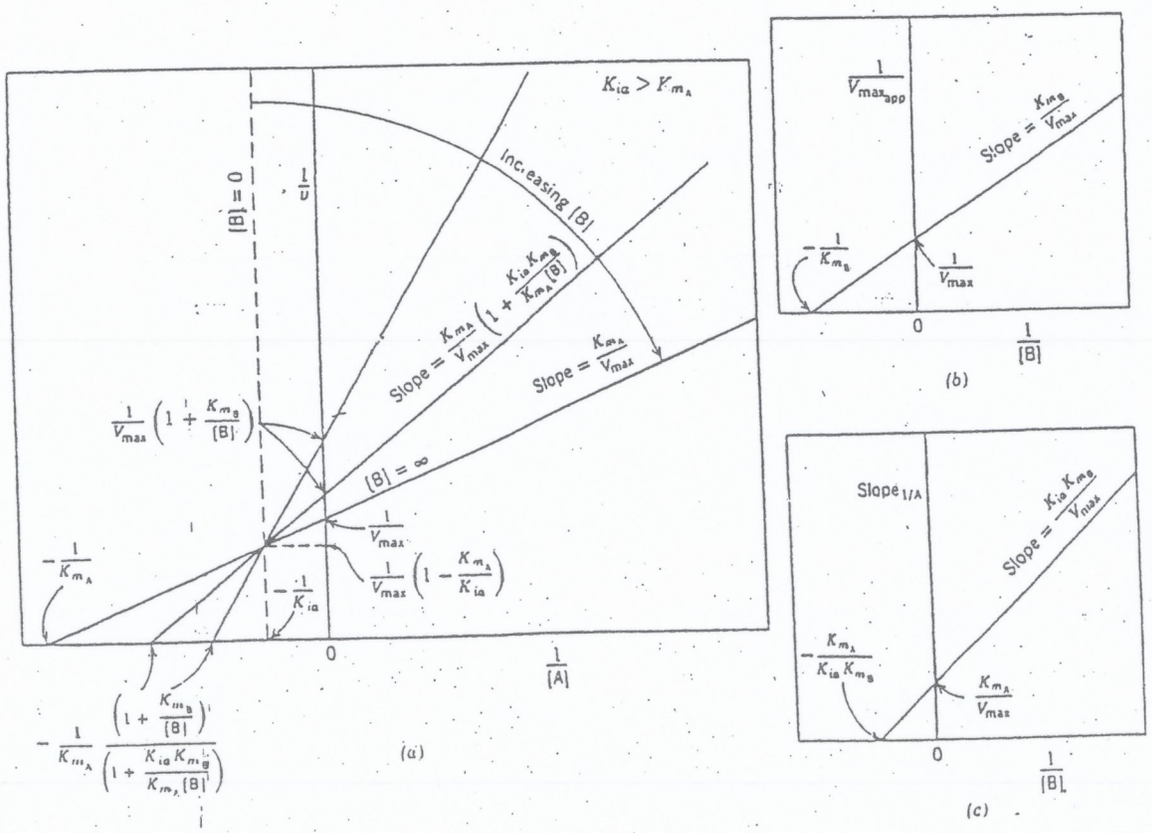
$K_{ia} > K_{m_A}$
Increasing [B]
$\frac{1}{v}$
$[B] = 0$
$[B] = \infty$
Slope $= \frac{K_{m_A}}{V_{max}}\left(1 + \frac{K_{ia} K_{m_B}}{K_{m_A}[B]}\right)$
Slope $= \frac{K_{m_A}}{V_{max}}$
$\frac{1}{V_{max}}\left(1 + \frac{K_{m_B}}{[B]}\right)$
$\frac{1}{V_{max}}$
$\frac{1}{V_{max}}\left(1 - \frac{K_{m_A}}{K_{ia}}\right)$
$-\frac{1}{K_{m_A}}$
$-\frac{1}{K_{ia}}$
$-\frac{\left(1 + \frac{K_{m_B}}{[B]}\right)}{\left(1 + \frac{K_{ia} K_{m_B}}{K_{m_A}[B]}\right)}$
0
$\frac{1}{[A]}$
(a)
$\frac{1}{V_{max_{app}}}$
Slope $= \frac{K_{m_B}}{V_{max}}$
$-\frac{1}{K_{m_B}}$
$\frac{1}{V_{max}}$
0
$\frac{1}{[B]}$
(b)
Slope $_{1/A}$
Slope $= \frac{K_{ia} K_{m_B}}{V_{max}}$
$-\frac{K_{m_A}}{K_{ia} K_{m_B}}$
$\frac{K_{m_A}}{V_{max}}$
0
$\frac{1}{[B]}$
(c)

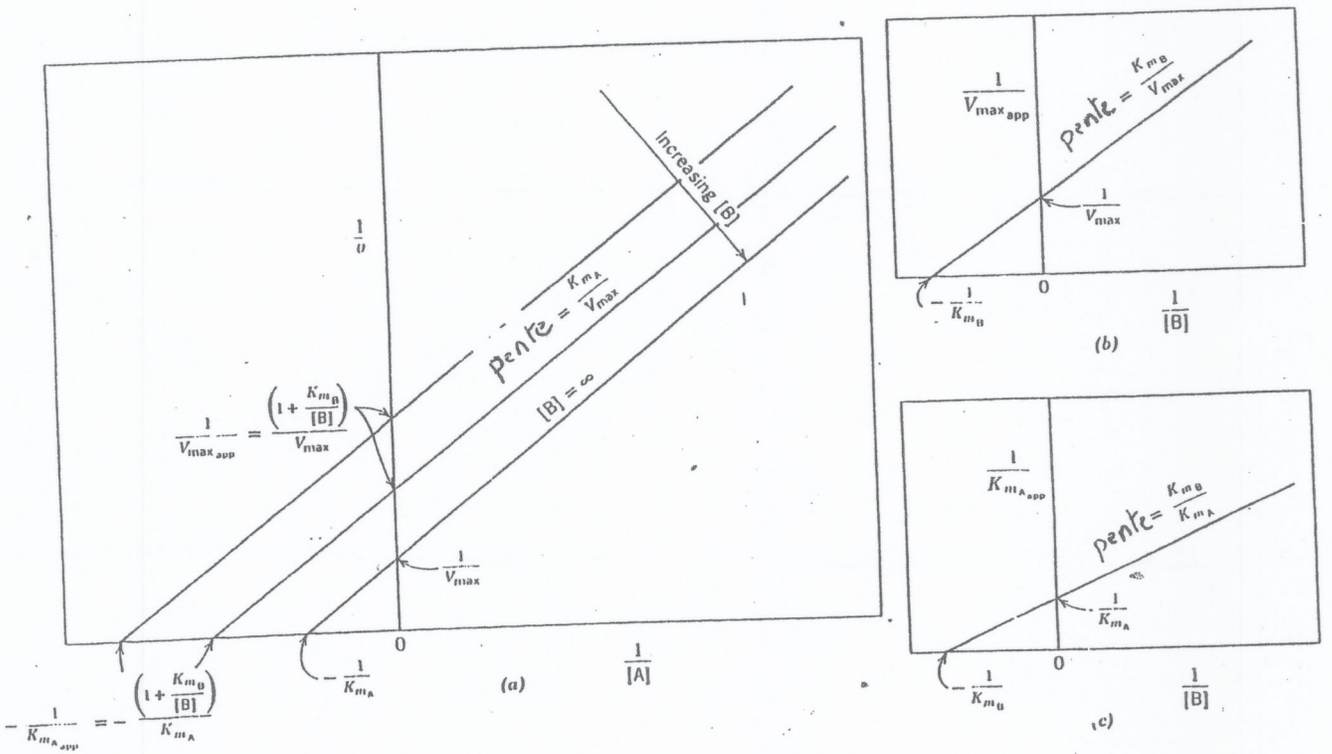
1/v
Increasing [B]
pente = Km_A / Vmax
[B] = ∞
1/Vmax app = (1 + Km_B/[B]) / Vmax
1/Vmax
0
1/[A]
(a)
-1/Km_A app = -(1 + Km_B/[B]) / Km_A
-1/Km_A
1/Vmax app
pente = Km_B / Vmax
1/Vmax
-1/Km_B
0
1/[B]
(b)
1/Km_A app
pente = Km_B / Km_A
1/Km_A
-1/Km_B
0
1/[B]
(c)

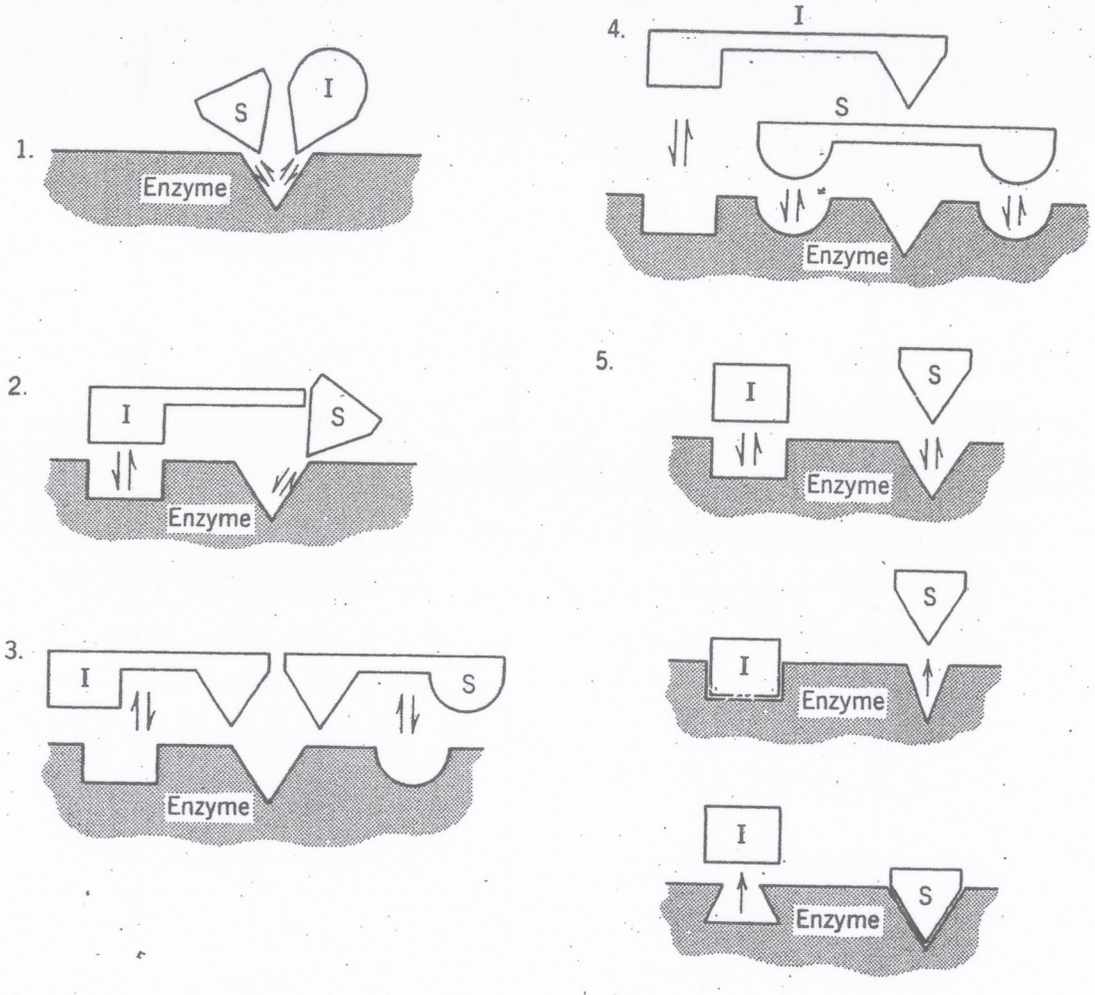

Figure Models of competitive inhibition: S and I are mutually exclusive. (1) Classical model. S and I compete for the same binding site. I must resemble S structurally. (2) I and S are mutually exclusive because of steric hindrance. (3) I and S share a common binding group on the enzyme. (4) The binding sites for I and S are distinct, but overlapping. (5) The binding of I to a distinct inhibitor site causes a conformational change in the enzyme that distorts or masks the substrate binding site (and vice versa).

Segel, 1976

1 Inhibition compétitive

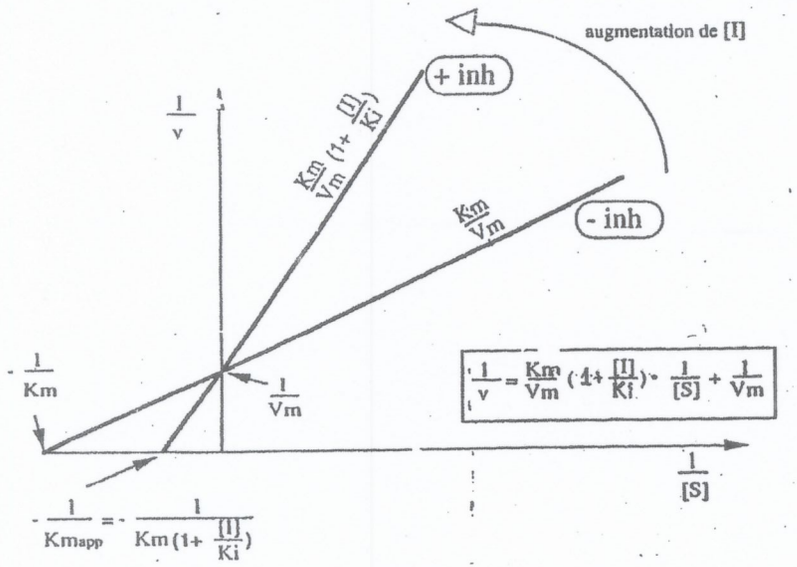

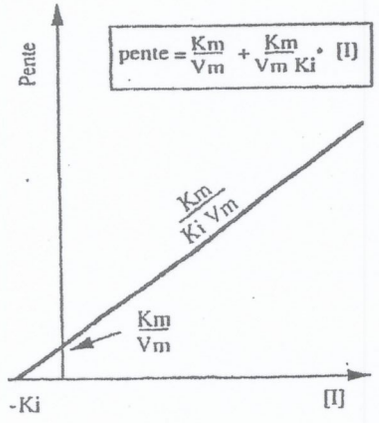

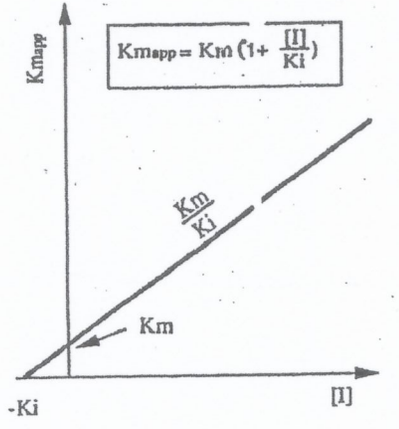

3. Inhibition acompétitive

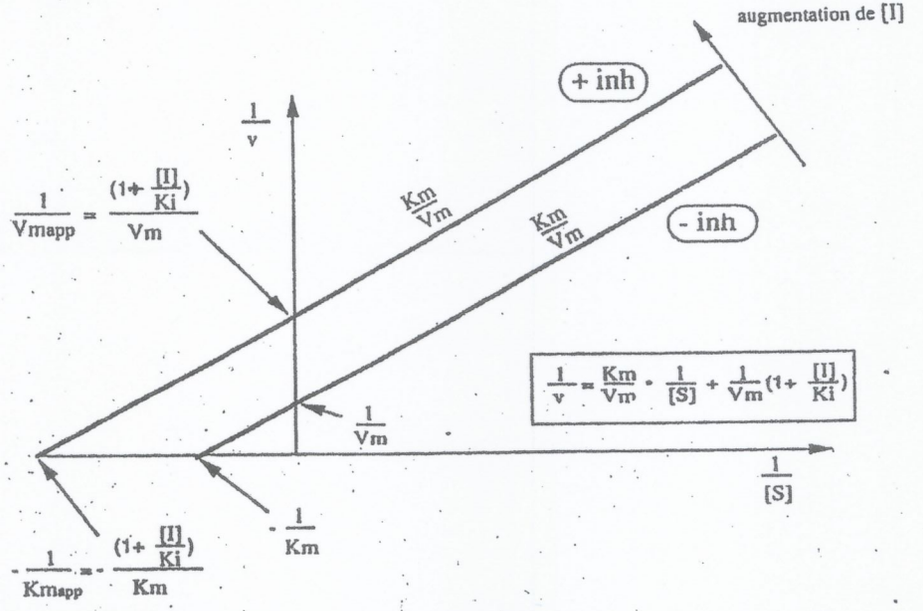

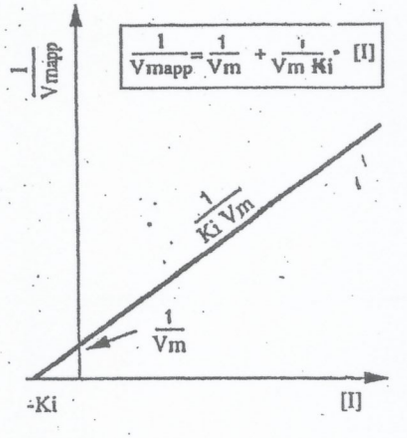

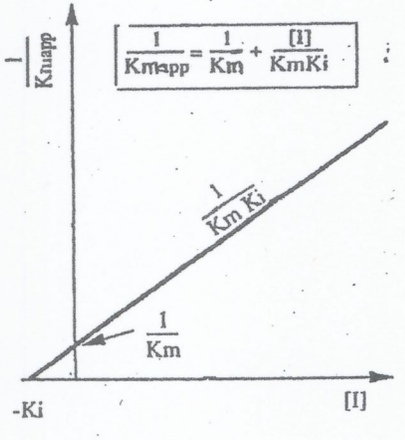

1' Inhibition non compétitive mixte

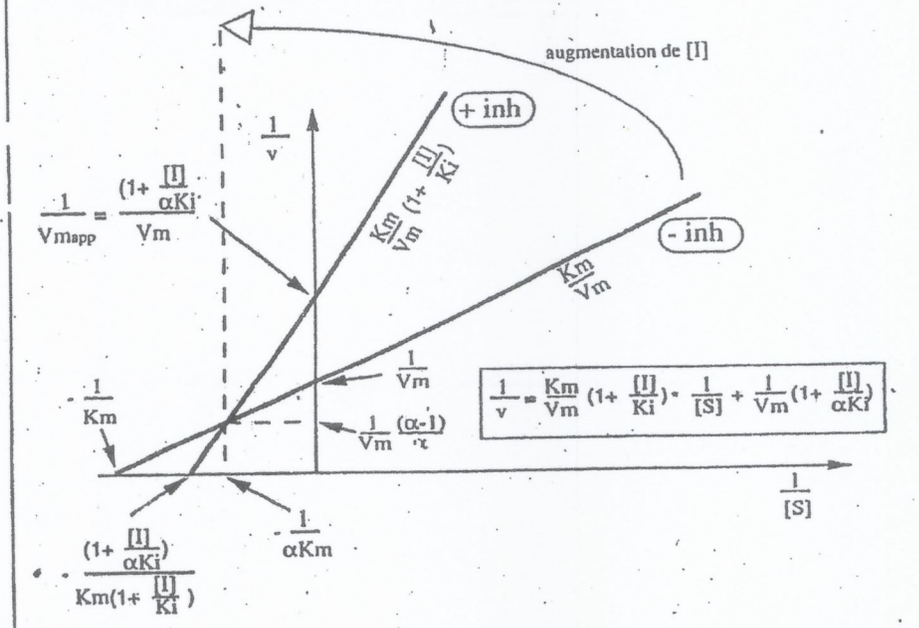

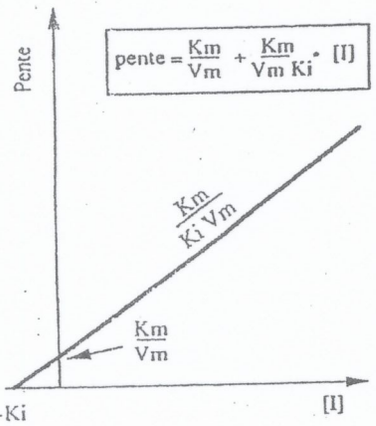

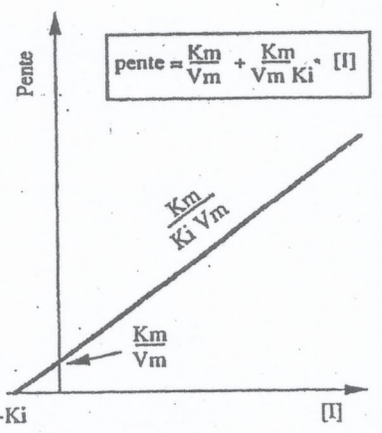

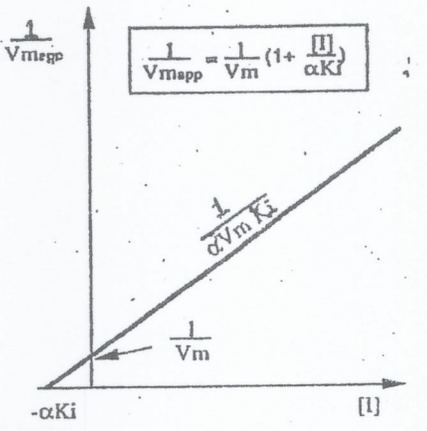

2 Inhibition non compétitive

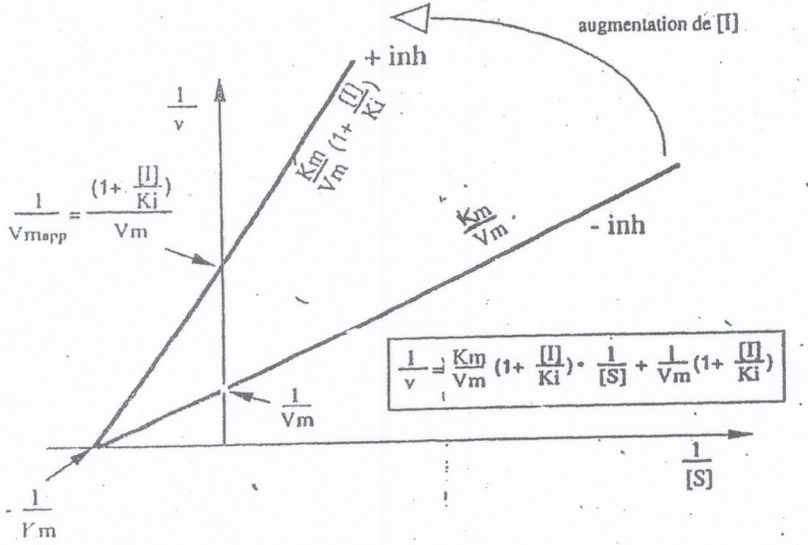

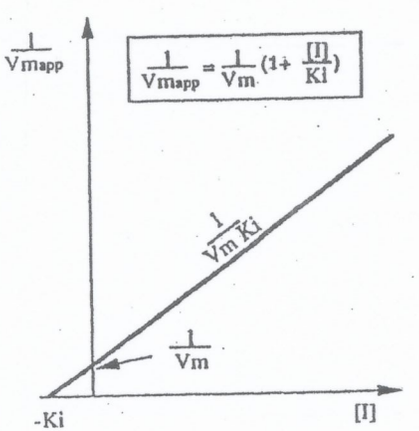

Table 5 Various Types of Substrate Analogs

Type (enzyme involved)	Substrate	Inhibitor
1. Enantiomeric analogs (ficin, papain)	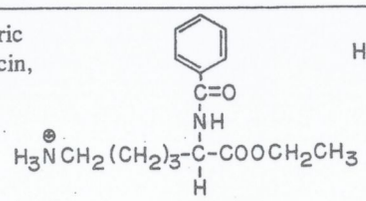 L-BLEE	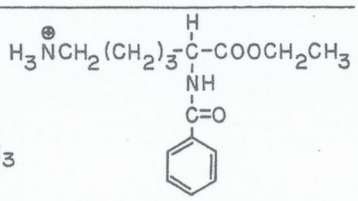 D-BLEE
2. Anomeric analogs (α-glucosidase)	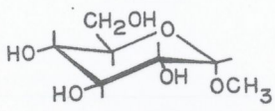 α-Methyl-D-glucose	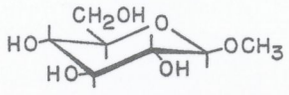 β-Methyl-D-glucose
3. Positional isomers (p-hydroxyphenyl pyruvate hydroxylase)	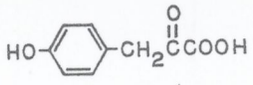 *p*-Hydroxyphenylpyruvic acid	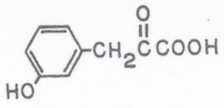 *m*-Hydroxyphenylpyruvic acid
4. Geometrical isomers (fumarase)	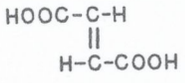 Fumaric acid	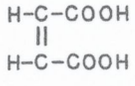 Maleic acid
5. Product of reaction (carboxypeptidase A)	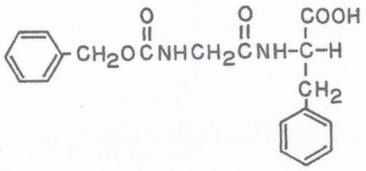 Benzyloxycarbonylglycyl-L-phenylalanine	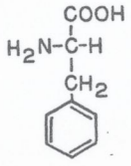 L-Phenylalanine
6. Compounds resembling substrate (enolase)	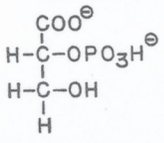 D-2-Phosphoglycerate	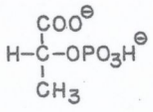 D-Phospholactate

Table 7 Inhibitors of Carboxypeptidase A

Compound	Structure	K_i (m*M*)
Propionate	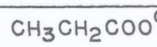	100
Valerate	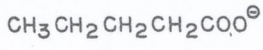	2.7
Benzoate	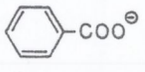	143
Phenylacetate	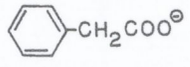	4.55
β-Phenylpropionate	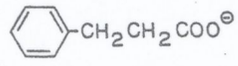	1.2
γ-Phenylbutyrate	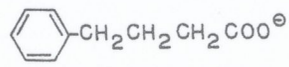	20
3-Indoleacetate	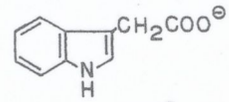	0.78
L-Phenylalanine[a]	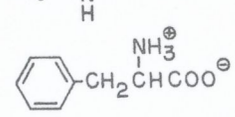	2.0
D-Phenylalanine[b]	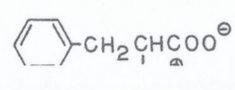	2.0

Whitaker, 1994

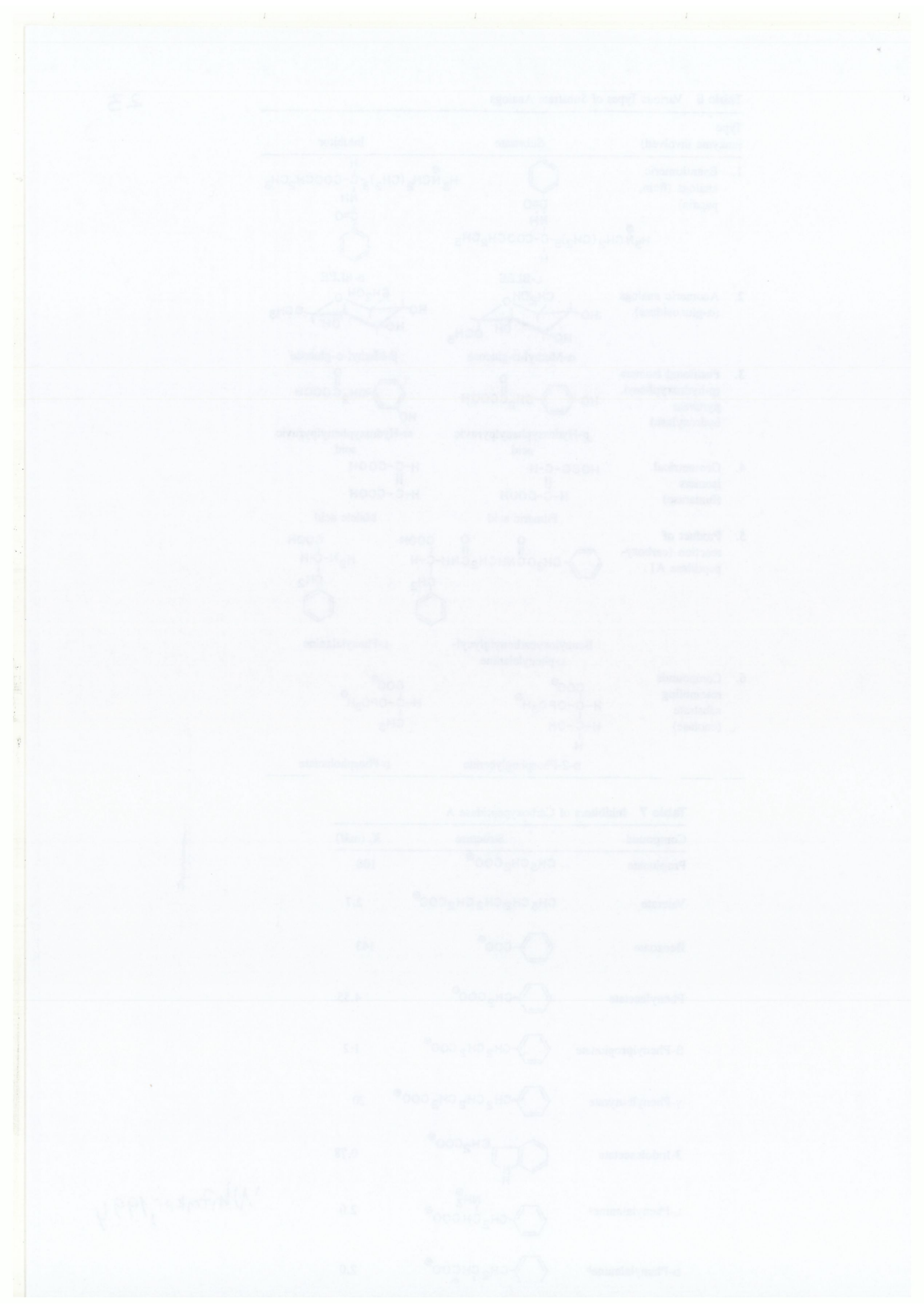

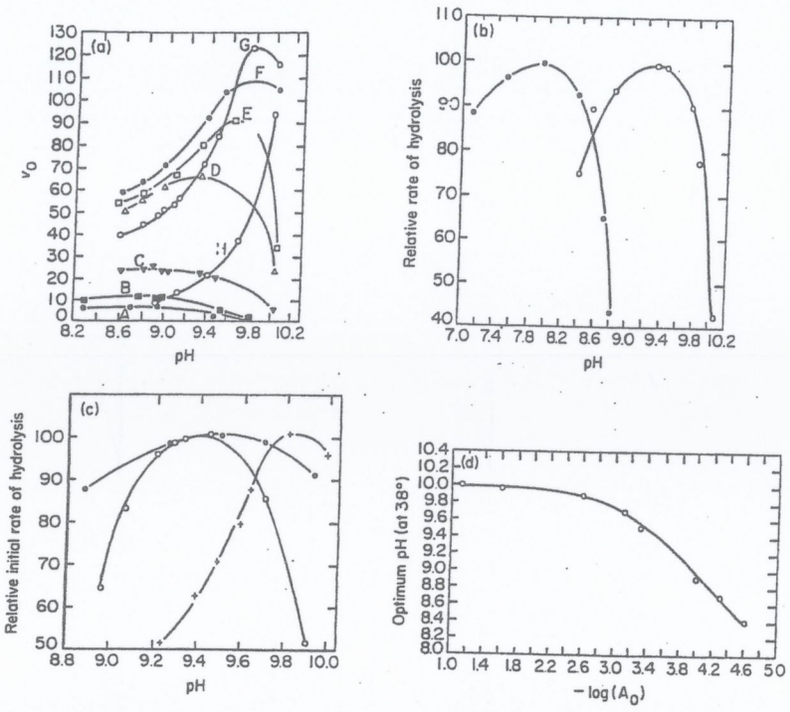

Figure 1 Effect of experimental conditions on the pH optimum of calf intestinal mucosa alkaline phosphatase. (a) Effect of initial substrate concentration on pH optimum. The curves are for the following substrate (phenyl phosphate) concentrations (*M*): A, 2.5×10^{-5}; B, 5×10^{-5}; C, 1×10^{-4}; D, 5×10^{-4}; E, 7.5×10^{-4}; F, 2.5×10^{-3}; G, 2.5×10^{-2}; H, 7.5×10^{-2}. (From Ref. 1, p. 675, by courtesy of the Biochemical Society.) (b) Effect of nature of activating cation on pH optimum. The cations were: ○, 5×10^{-3} *M* $MgCl_2$ and ●, 1×10^{-3} *M* $MnCl_2$ with 2.5×10^{-4} *M* phenyl phosphate as substrate. (From Ref. 1, p. 677, by courtesy of the Biochemical Society.) (c) Effect of nature of substrate on pH optimum. The substrates were: ●, 0.015 *M* phosphocreatine; ○, 0.02 *M* β-glycerophosphate; +, 0.025 *M* phenyl phosphate. (From Ref. 2, p. 235, by courtesy of the Biochemical Society.) (d) pH optima from data of part (a) plotted against $-\log(A_0)$. The lowest substrate concentration is at the right of the figure. (From Ref. 1, p. 675, by courtesy of the Biochemical Society.) The temperature was 38.0°C in all cases.

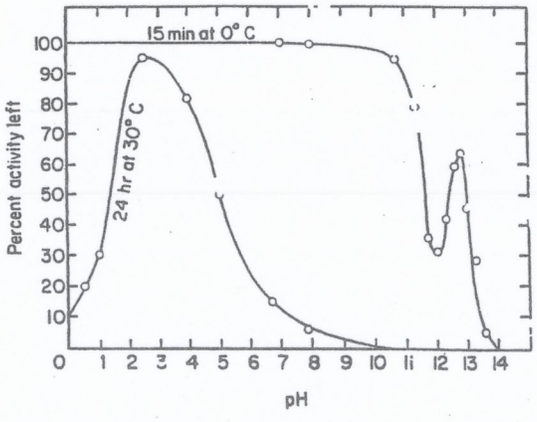

Figure 3 pH stability of trypsin under two sets of conditions. courtesy of Columbia University Press.)

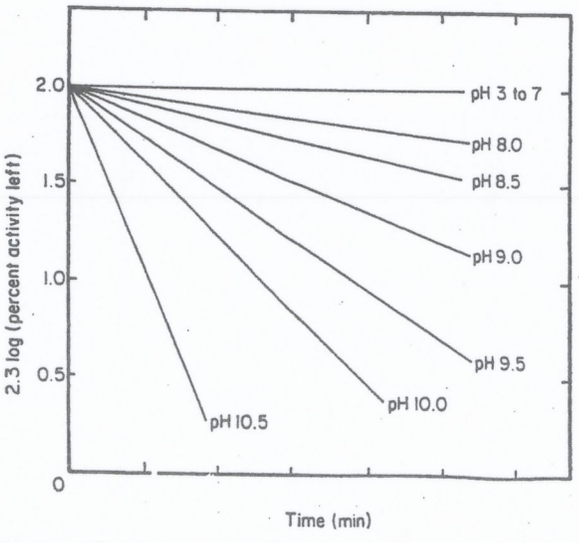

Figure 5 Schematic representation of rates of inactivation of an enzyme incubated at different pH values.

Whitaker, 1994

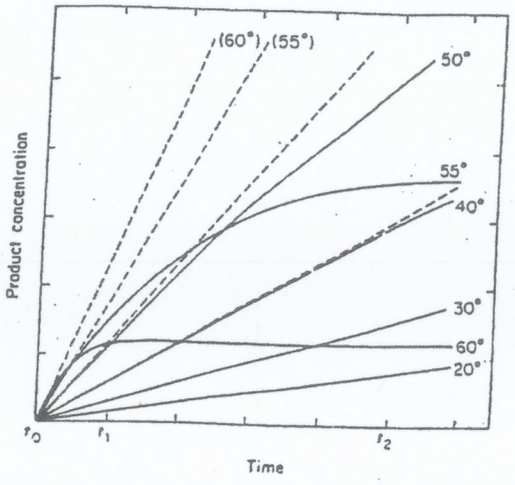

Figure 1 Effect of temperature on rate of product formation. The solid lines are for experimental data; the dashed lines are based on initial rates (i.e., lines drawn tangent to experimental data at time = 0). The data shown were calculated for the following

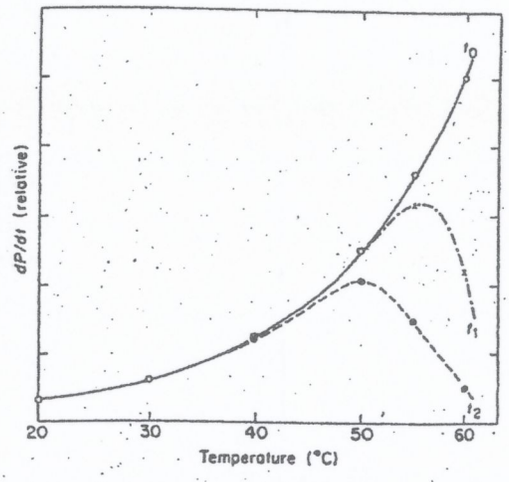

Figure 2 Rate of formation of product as function of temperature. Data taken from Fig. 1 at t_0, t_1, and t_2 are plotted, where t is time.

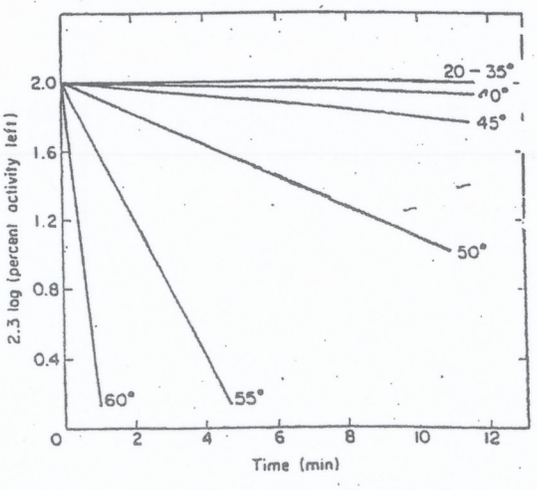

Figure 3 Rate of denaturation of an enzyme at various temperatures. The data are calculated for E_u of 60,000 cal/mol, where the first-order rate constant, k, of denaturation is 0.005, 0.020, 0.090, 0.395, and 1.80 min^{-1} at 40, 45, 50, 55, and 60°C, respectively.

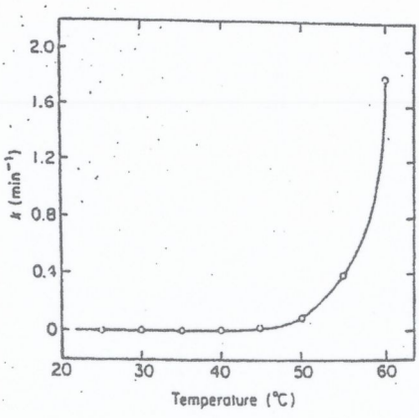

Figure 4 Effect of temperature on stability of an enzy

The first-order rate constants, k, from fig 3 are plotted as a function of temperature